Extragalactic Background Light and Extragalactic Magnetic Fields

Andrew M. Taylor

ISDC Data Centre for Astrophysics, University of Geneva, Switzerland
Dublin Institute for Advanced Studies, 5 Merrion Square, Dublin 2, Ireland

Abstract. VHE γ-rays from distant blazars several hundred Mpc away are attenuated through pair production interactions on extragalactic background light (EBL). Subsequent to their generation, electron/positron pairs proceed to produce γ-rays through IC interactions leading to the development of an electromagnetic (EM) cascade. Due to the deflection of VHE cascade electrons by extragalactic magnetic fields (EGMF), the spectral shape of this arriving γ-ray emission is dependent on the strength of the EGMF. The GeV-TeV spectral shape of blazars has, thus, the potential to probe the EGMF strength along the line of sight to the object. Focusing on the specific example cases of the blazar 1ES 0229+200 and PKS 2155-304, bounds on the EGMF are obtained using both the spectral and angular observational information from the these two blazars.

Keywords: Blazars, Electromagnetic Cascades, EGMF
PACS: 95.85.Sz, 98.54.Cm,

1. INTRODUCTION

Magnetic fields in galaxies and galaxy clusters play a key role in present day astrophysical studies. However, the origin of these fields remains largely unknown (see [1, 2, 3, 4] for reviews). The current working hypothesis, however, is that relatively strong galactic and cluster magnetic fields result from the amplification of much weaker pre-existing "seed" fields via compression and turbulence/dynamo amplification in the course of the structure formation process [5]. The present uncertainty in the strength of these extragalactic magnetic fields remains significant.

In this proceeding we investigate a promising new probe of the extragalactic magnetic field (EGMF) utilising the phenomena of electromagnetic (EM) cascades. Focusing specifically on two architypal blazars as examples, the energy and spatial distribution of their very high energy γ-ray emission is analysed. The results from this analysis is used to derive interesting new constraints on the EGMF, which prior to the use of this effect had been left almost wholly unconstrained.

The layout of this proceedings is the following. In section 2 a summary of the observational status of the EGMF is briefly reviewed. In section 3 a description of the physics behind EM cascades in discussed. Following this, a simplified "2 generation" model of these cascades which incorporates the key physics in discussed in section 4. In section 5.1, the spectral shape of the blazar 1ES 0229+200 is analysed to look for evidence of cascade spectrum signatures in the SED. Lastly, in section 5.2, the angular profile of the blazar PKS 2155-304 is studied to look for evidence of angular broadening by the EGMF. A summary of our conclusions are given in section 6.

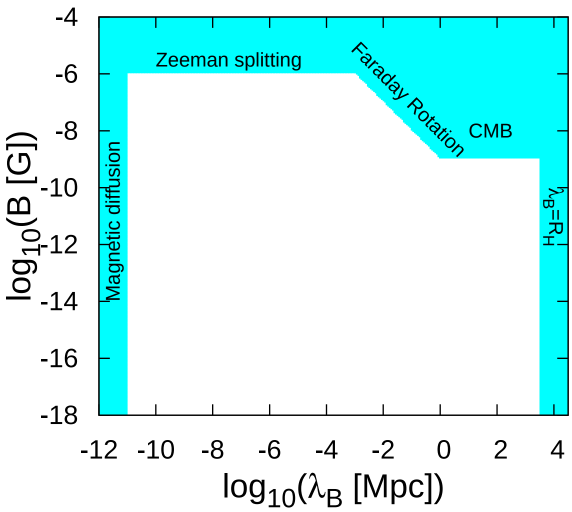

FIGURE 1. A λ_B-B diagram showing the regions of EGMF parameter space excluded by present observational constraints. The white regions in the plot highlight the regions still allowed whilst the blue regions highlight those that are excluded.

2. EXTRAGALACTIC MAGNETIC FIELDS

The measurement of extremely weak magnetic fields in the voids of the Large Scale Structure (LSS) is a challenging task and up until recently only upper bounds have been derivable using various techniques. Of these techniques, the tightest upper bounds come from the search for the Faraday rotation of polarised radio emission from distant quasars [6, 7, 8] and from the effect of magnetic fields on the anisotropy of Cosmic Microwave Background radiation [9, 10]. A plot summarising the observational status of the EGMF from the discussion above is provided in Fig. 1.

However, in recent years a new handle on the EGMF, using the cascade emission from blazars, has started to emerge as an alternative probe. In this method, multi-TeV γ-rays from distant ($>$ 100 Mpc) blazars attenuate through pair production interactions on the extragalactic background light (EBL), and lead to the development of EM cascades [11, 12, 13, 14, 15, 16, 17, 18, 19]. The energy spectrum along different lines of sight to the blazar produced by the secondary cascade e^+e^- pairs deposited in the intergalactic medium through pair production interactions depends on the EGMF strength. The detection (non-detection) of the cascade emission signal from known TeV γ-ray emitting blazars could result in the measurement of (lower bound on) the strength of magnetic field pervading intergalactic space along the line of sight toward these blazars. The first application of this new method for deriving lower bounds on the EGMF have been carried out [20, 21, 22, 23], suggesting that a measure of the EGMF may finally soon be within reach.

An important ingredient in these calculations is the level and spectral shape of the EBL. The uncertainty in this quantity, however, is considerably smaller than that of the EGMF. As a fiducial model, we adopt the spectral shape of the model put forward in ref. [24], altering the normalisation of this model in order to investigate the subsequent effect this has on the EGMF bound obtained.

As well as altering the energy spectrum of particles in an EM cascade, the presence of the EGMF can also effect the angular profile of the cascade. The charged component in the cascade respond to the presence of the EGMF and gyrate around the field lines. Since the particles subsequently pass their energy back the photon population, the overall cascade subsequently becomes broader, an effect which is energy dependent.

3. ELECTROMAGNETIC CASCADES

Frequently, for EBL studies, the assumption that the multi-TeV γ-ray flux from distant blazars is attenuated following the simple relation,

$$\frac{dN_\gamma}{dE_\gamma}_{\rm arr} = e^{-\tau} \times \frac{dN_\gamma}{dE_\gamma}_{\rm source} \tag{1}$$

where dN_γ/dE_γ describes the γ-ray flux and τ is the γ-ray photon optical depth between the source and Earth.

This simple attenuation expression, however, is only applicable if the subsequent energy flux, once passed on to the electron/positron pairs, can be safely neglected thereafter. Though this is expected to be the case for sufficiently strong EGMF, which would sweep the low energy electrons out of the line of sight, more generally such an assumption is unjustified. Indeed for weak EGMFs, the energy flux passed onto the electrons (and positrons) will continue to propagate in the forward direction, and may thus proceed to feed back into the γ-ray population through IC interactions. Consequently, for the general case of weak EGMF values, a pair of coupled differential equations describing both the photon and electron populations must be considered, of the form

$$\frac{dN_\gamma(E_\gamma)}{dt} + \frac{N_\gamma(E_\gamma)}{\tau_{\gamma\gamma}} = \frac{N_e(E_e)}{\tau_{e\gamma}} \tag{2}$$

$$\frac{dN_e(E_e)}{dt} + \frac{N_e(E_e)}{\tau_{e\gamma}} = \frac{N_\gamma(E_\gamma)}{\tau_{\gamma\gamma}} + \frac{N_e(E_e')}{\tau_{e\gamma}'}. \tag{3}$$

The frequency with which very high energy (VHE) electrons and photons interact with the background radiation fields is dictated by the corresponding cross-sections for these two processes shown in Fig. 2. From this plot two distinct center-of-mass regions are observed to exist for EM cascade development. Well above threshold ($s_{\rm th}^{1/2}/2m_ec^2 = 1$) the IC and pair-production cross-sections start to have the same functional form and for the same center-of-mass energy ($s^{1/2}$) their respective normalisations are only separated by a factor of two in value. Below threshold, however, the pair-production process switches off and the IC cross-section asymptotes to the Thomson cross-section value.

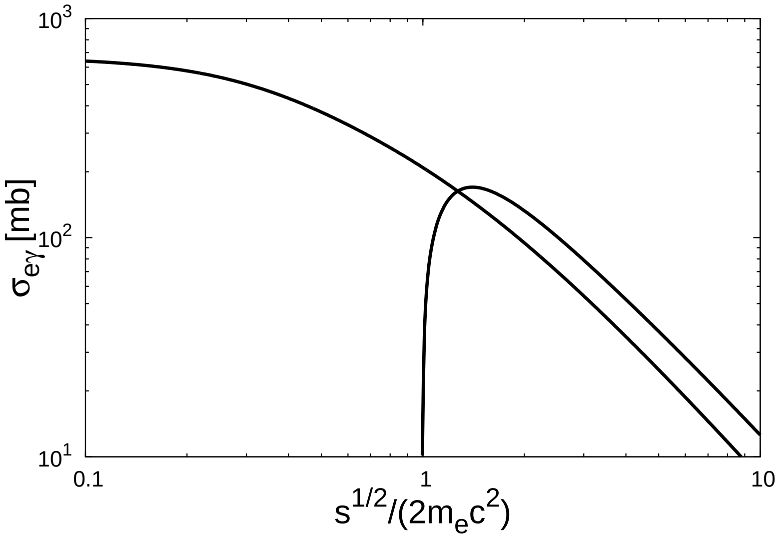

FIGURE 2. The inverse Compton and pair production cross-sections appropriate for very high electron and photon propagation respectively.

Considering the two center-of-mass regions, above and below threshold, the development of an EM cascade can be explained through a simple 2 region model. Assuming that the photons which initiate the cascade are well above threshold, the center-of-mass energies probed by the proceeding cascade particles (electrons and photons) lie to the right of $s_{\rm th}^{1/2}/2m_ec^2 = 1$ in Fig. 2. However, as the number of particles in the cascade increases, the energy per particle decreases (energy flux being the conserved quantity). Eventually, the photons start to interact close to threshold, and the subsequent electrons (and positrons) produced begin to probe the cross-section below $s_{\rm th}^{1/2}/2m_ec^2 = 1$. The IC photons produced by these electrons now have insufficient center-of-mass energy to pair-create, and the energy flux in the cascade is passed back by the electrons (and positrons) to photons.

In order to track the development of the photon and electron populations for the calculations carried out in this work, we employ a Monte-Carlo description of the EM cascade development in order to determine the arriving spectra observed for the case of a given strength EGMF (see [25] for more details). For these calculations, the shape of the EBL spectrum was assumed to follow that derived by [24], while the normalization of the EBL was left free in order that the dependence of the EGMF bound on the EBL normalisation could be investigated. With regards the normalisation range probed in this work, a lower bound on the normalization of the EBL from the direct source counts (as summarized by [26]) is $\simeq 15\%$ lower than the normalization of the EBL model of [24]. Recent analysis of GeV to TeV spectra of sevearal blazars ([27]), however, suggested that the EBL level is somewhat higher, reaching $\simeq 60\%$ of the EBL model of [24] at the 2σ confidance level. In this work we thus scanned over the EBL normalisation in the range 0.85-1.6.

In our calculaitons for obtaining a bound on the EGMF strength, we consider suppression of the cascade emission by the time delay of the cascade signal ([12]). The TeV

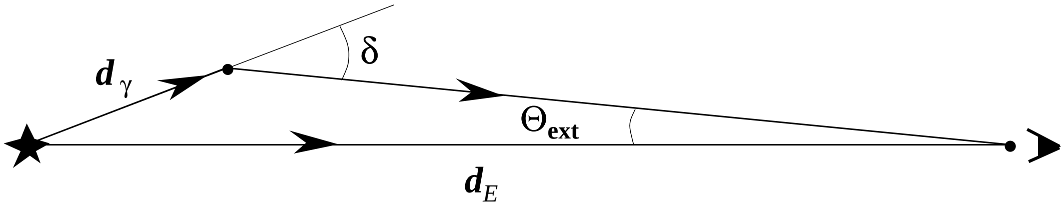

FIGURE 3. A depiction of the “2 generation” model, taken from [28].

γ-ray emission from the source (1ES 0229+200) is observed to be stable on the time scale of ≥ 3 yr, from the initial HESS observations of the source ([29]) till the recent re-observation by the Veritas telescope ([30]). We thus adopt a stability timescale of 3 yrs for the blazar in our EGMF bound calculations.

We note, however, that an alternative possibility for the suppression of the cascade flux is that the suppression comes about from the cascade emission becoming extended in nature. As was discussed in [25, 31], such a possibility requires stronger EGMF values (by about 2 orders of magnitude) than those required for the temporal suppression effect. Interestingly, such a scenario would itself also imprint a unique signature on the observed cascade through a dependence of the angular extension of the blazar on the γ-ray energy. In this way a search for such a signature in the angular information from the blazar may be used to constrain the EGMF strength in a different region of parameter space to that probed by the temporal suppression effect discussed previously.

4. SIMPLIFIED 2 GENERATION MODEL

The Monte Carlo description of EM cascades through a non-negigible EGMF described in the previous section provides a complete description of these phenomenon. However, in anticipation of the benefits provided by a simplified picture to facilitate an understanding of the results obtained from the Monte Carlo, a complementary analytic model encapsulating the essence of the Monte Carlo description is outlined below.

For such a toy model, we discuss here a simplified “2 generation” cascade, in which primary VHE photons interact close to threshold with EBL photons, producing secondary electron/positron pairs which themselves interact with CMB photons generating secondary photons which can contaminate the primary beam. A diagram depicting this simplified set-up is shown in Fig. 3, in which the blazar is on the far left of the image and the observer is on the far right.

Using Fig. 3, a useful expression for the typical secondary time-delay that cascade photons can be expected to arrive with relative to that of the primary photons may be derived,

$$t_{\rm delay} \approx \delta^2 \left(\frac{d_\gamma}{c}\right), \tag{4}$$

for $d_E \gg d_\gamma$ and $\delta \ll 1$. Since $\delta \approx c t_e^{\rm cool}/R_{\rm Larmor}$, it follows that $\delta \propto E_e^{-2} \propto E_\gamma^{-1}$. Numerical verification of this dependency, obtained by the application of the full Monte

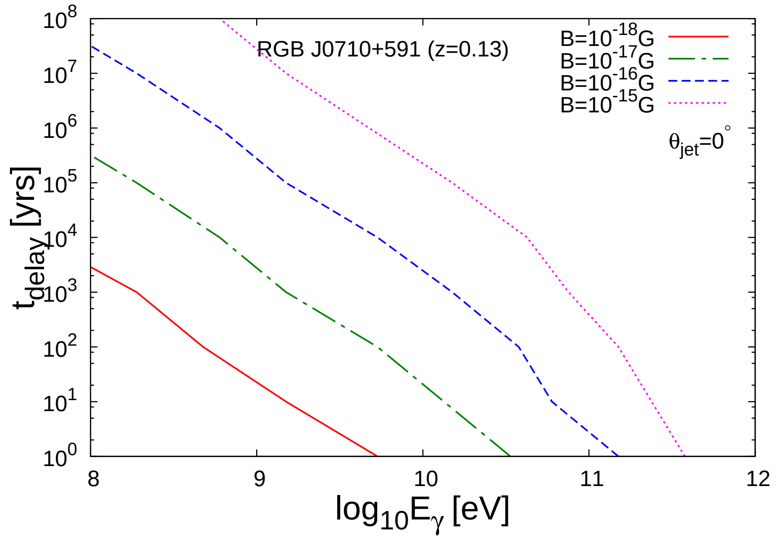

FIGURE 4. Verification of relation (4) for the case a blazar at redshift 0.13. This result has been taken from [25].

Carlo description, is shown in Fig. 4. An understanding of this time-delay effect will be of benefit for the proceeding section.

5. RESULTS

5.1. 1ES 0229+200

Constraints on the intrinsic slope of the spectra of blazars can be obtained from the observations by the Fermi Large Area Telescope (LAT) ([32]) in the energy band below $\sim$ 100 GeV, where the effect of absorption on the EBL becomes negligible. However, the blazars used for the derivation of constraints on the EBL are characterized by hard spectra, which makes it difficult to observe their flux below 100 GeV. In fact, the blazar 1ES 0229+200, which provides the tightest constraints on the EBL ([29]) was not listed in the two-year exposure catalogue of sources detected by LAT ([33]), with only upper limits on the source flux derived from the LAT data ([20, 25]) and a weak detection reported by [27].

The blazar 1ES 0229+200, however, was eventually detected by LAT in the 1-300 GeV energy band with a significance $\simeq 7\sigma$ after three years of exposure. The test statistics (TS) value found in the likelihood analysis was $TS = 45$. Modeling the source spectrum as a powerlaw we find the slope of the spectrum $\Gamma = 1.36 \pm 0.25$ and normalization at 20 GeV $(1.4 \pm 0.5) \times 10^{-15}$ (MeV$\cdot$cm$^2\cdot$sec)$^{-1}$ (at the 68% confidence level). The spectrum of the source found from the LAT data is shown in Fig. 5 together with the HESS spectrum at higher energies. The source was not detected below $\simeq$ 3 GeV, with only an upper limit on the source flux being derived in this energy band.

Employing our simplified “2 generation” picture discussed in section 4, the source

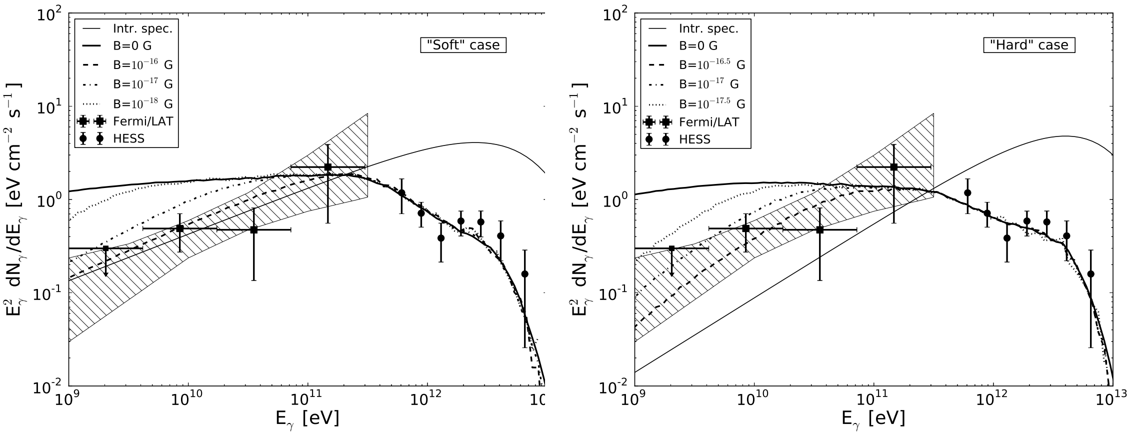

FIGURE 5. Left-hand panel: the GeV-TeV SED under the assumption of a soft ($\Gamma = 1.5$) intrinsic source spectrum. Right-hand panel: the GeV-TeV SED under the assumption of a hard ($\Gamma = 1.2$) intrinsic source spectrum. In both cases the Fermi/LAT flux "butterfly" shown corresponds to the 68% confindence region. These results have been taken from [34].

spectrum in the 3-300 GeV energy band can have two possible contributions: the direct γ-ray signal from the primary source and emission from the EM cascade developing in the IGM. It is not clear a-priori if the measured spectral slope, consistent with $\Gamma \simeq 1.5$, characterizes the intrinsic source spectrum, the spectrum of the cascade component, or comprises an average spectrum of the two (similar in strength) contributions. The different possibilities for the dominance of one of the two components in the spectrum are illustrated in the two panels of Fig. 5. In both models we assume that the intrinsic source spectrum has a high-energy cut-off at $E_{cut} = 5$ TeV. It was shown by [25], that this choice minimizes the strength of the cascade contribution in the Fermi/LAT energy band.

In the left-hand panel of Fig. 5 the main contribution to the 3-300 GeV source flux is given by the direct flux of the primary source, shown by the thin solid line. This is possible only if the cascade component is suppressed by the influence of a strong enough EGMF. If the EGMF is negligible, the flux of the cascade component (thick solid line) will largely dominate over the direct emission in this energy range. Strong EGMF ($\geq 10^{-17}$ G) is needed to sufficiently suppress the cascade emission down to the level of the errorbars of the LAT measurements in the 3-300 GeV range.

If the EGMF is weaker than $\sim 3 \times 10^{-18}$ G, the cascade emission provides the dominant contribution to the source spectrum, as is illustrated in the right-hand panel of Fig. 5. The only possibility to make the LAT measurement consistent with observations is to assume that the intrinsic spectrum of the primary source has a slope harder than $\Gamma = 1.5$. The hardness of the intrinsic source spectrum depends on the EGMF strength. For the particular example shown in the right-hand panel of Fig. 5, the assumption that the EGMF strength $B \leq 3 \times 10^{-18}$ G imposes a constraint on the intrinsic source spectrum $\Gamma \leq 1.2$. In fact, if the intrinsic source spectrum is still harder, the intrinsic source flux contribution to the 3-300 GeV band flux becomes negligible and the flux is completely dominated by the cascade emission.

The overall normalization of the cascade emission is determined by the density of

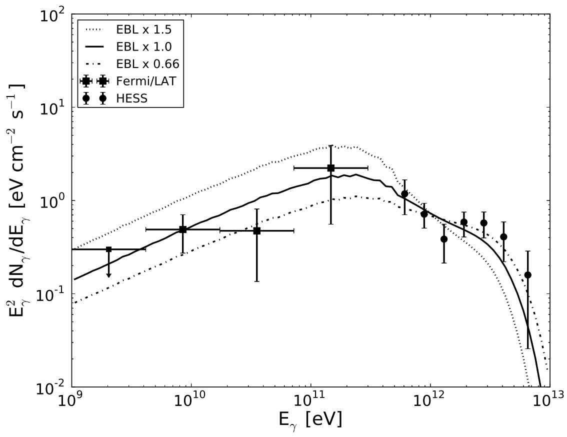

FIGURE 6. GeV-TeV SED under the assumption of a soft ($\Gamma = 1.5$) intrinsic spectrum for different EBL normalisations. The reference EBL scale is that of [24]. This result has been taken from [34].

the EBL. An increase of the EBL density leads to stronger absorption of multi-TeV γ-rays and, consequently, to stronger cascade emission. To the contrary, reducing the EBL normalization down to the level of the lower bound from the direct source counts opens up the possibility of a somewhat weaker EGMF, down to $\sim 10^{-18}$ G. The effect of changing the EBL normalization is illustrated in Fig. 6. In this figure a spectral slope of $\Gamma = 1.5$ and EGMF of 10^{-16} G have been adopted, and the level of EBL has been altered.

The maximal normalization of the EBL which can still be consistent with the data depends on the EGMF strength. Too strong an EBL can result in a large over-prediction of the strength of the cascade emission, even after taking into account the suppression of this emission by the EGMF effects. Thus, the upper bound on the EGMF derivable from the γ-ray observations of 1ES 0229+200 is strongly EBL dependent.

The EGMF dependent EBL upper bound is shown in Fig. 7 in which the hatched region depicts the excluded region found in this work. The two exclusion fronts shown are for the 99.7% and the 95% C.L respectively (from left to right). One can see from this figure that for EGMF strengths $B \sim 10^{-17}$ G the upper bound sits at the level of [24]. If the EGMF is at the level of $\sim 10^{-15}$ G, the allowed EBL normalization is by a factor of 2 higher than that of the [24] and [26] models.

An asymptotic trend of the exclusion boundary is noted to occur for strong ($> 10^{-17}$ G) EGMF values, as can be seen in Fig. 7. The origin of this trend may be understood through an application of the "2 generation" model described in section 4. As was mentioned in section 3, our bound on the EGMF follow from the observed constraint that the blazar is approximately steady on a 3 yr timescale. An expression for the dependence of this time delay on d_γ and δ was given in eqn (4). Thus, the time delay depends both on the EGMF and EBL strengths, and for a given time delay a stronger EBL requires a stronger EGMF. This (qualitatively at least) explains the asymptotic nature of the bound for strong EGMFs.

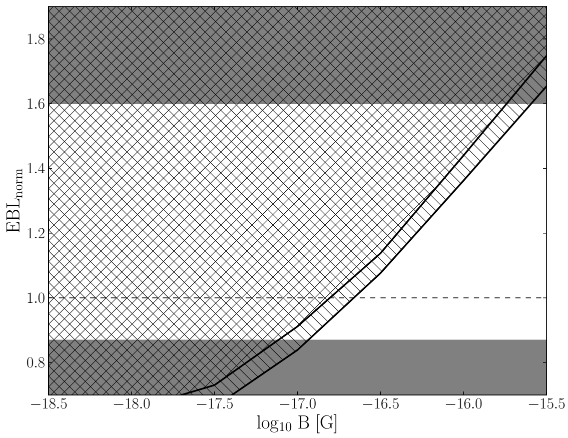

FIGURE 7. An EBL normalisation/EGMF strength exclusion plot. The reference EBL scale is that of [24]. The two exclusion bands, from left to right, are for the 99.7% and 95% C.L. respectively. This result has been taken from [34].

5.2. PKS 2155-304

One of the brightest known blazars, PKS 2155-304 has been observed in the $>$ 300 GeV range by the HESS Cherenkov telescope array for more than a total of 150 hours. Such a large accumulation of γ-rays from one particular blazar provides an ideal opportunity for angular distribution studies.

Employing the simplified "2 generation" model discussed in section 4, the degree of angular spread expected to be introduced via the presence of non-negligible EGMF is,

$$\delta \approx ct_e^{\rm cool}/R_{\rm Larmor} \approx 0.3^\circ \left(\frac{E_e}{10~\rm TeV}\right)^{-2}\left(\frac{B}{10^{-15}~\rm G}\right). \qquad (5)$$

This estimated value for the deflection, in fact, agrees very well with the more detailed Monte Carlo result. This result indicates that for Cherenkov telescopes with an angular resolution of $\sim 0.1^\circ$, EGMF strengths in the fG range can be expected to be probeable through angular broadening studies.

Utilising our Monte Carlo description of EM cascades developed in [25], the expected angular profile of the cascade emission from PKS 2155-304 was determined for different EGMF strengths.

In Fig. 8 the 0.3 – 1 TeV angular profiles of the resultant beam broadened cascades are shown for the case of PKS 2155-304. As seen from this figure, the large number of statistics available for PKS 2155-304 provide some discrimination power for EGMF constraints to be made from the angular information.

For this object, a significant cascade contribution results from the required high energy cutoff for which a conservative value of 10 TeV was adopted. Furthermore, a relatively soft spectral index of $\Gamma = 1.8$ was used in order to find consistency with recent Fermi measurements and at the same time minimise the energy flux injected into the EM cascade. For this case, the beam broadening introduced by fields of strength 10^{-15} G or a factor of a few stronger is in conflict with the H.E.S.S. measurements, at the 99.5%

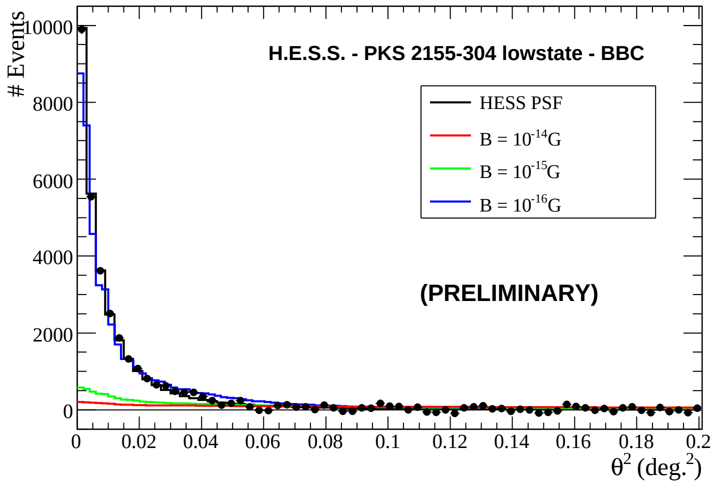

FIGURE 8. The angular profile of the blazar PKS 2155-304 observed during a low-state by the HESS Cherenkov telescope array. Due to the strong energy dependence of electrons in an EM cascade, only γ-rays in 300 GeV-1 TeV band have been selected. The lines shown are the MC calculated angular profiles of EM γ-rays expected for their respective EGMF strengths, assuming a coherence lengths of 1 Mpc.

C.L. However, for sufficiently strong fields, $> 3 \times 10^{-15}$ G, the cascade component becomes significantly reduced by spatial suppression effects, such that it sits below the level of that expected from the direct emission component, reducing the subsequent angular spreading back to that of the H.E.S.S. PSF. Thus, using the angular profile of the blazar PKS 2155-304, an EGMF in the range $1 - 3 \times 10^{-15}$ G is excluded at the 99.5% C.L. We note that for a larger cutoff energy than the conservative value considered here, the range of excluded EGMF would be a few times larger.

6. CONCLUSION

Our knowledge as the presence of the EGMF remains a highly unconstrained domain in astrophysics, as indicated by Fig. 1. Only in recent years, through the development of ground-based and space-based γ-ray astrophysics has new light begun to be shed onto this long standing problem.

For very high energy γ-ray photons produced by AGN several hundred Mpc away, the extragalactic space between these blazars and Earth is optically thick. EBL photons pervading this space provide the dominant target and hinder the propagation of multi-TeV photons through pair production interactions.

For the case in which no significant EGMF fields exists, the absorbed component of the injected spectrum photons, through their pair production interactions with EBL photons, is reprocessed through the development of an EM cascade through the repetition of pair production and inverse Compton scattering interactions. The development of such a cascade leads to the production a relatively flat (when view in the energy flux representation) spectrum at energies below 200 GeV. Examples showing this result are shown

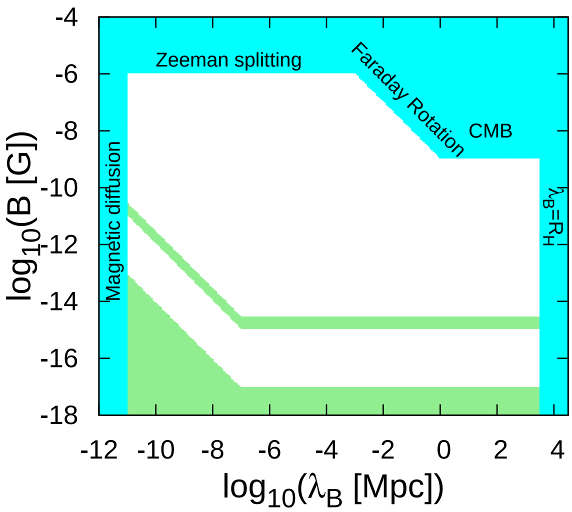

FIGURE 9. An updated version of the λ_B-B diagram showing the excluded EGMF regions subsequent to these blazar studies. The white regions in the plot highlight the regions still allowed whilst the blue regions highlight those that are excluded. The additional green regions indicate the new excluded regions following the electromagnetic cascade studies carried out in this work.

as the $B = 0$ G line in both plots of Fig. 5. The observation of blazars whose spectra show little evidence of a cutoff up to the highest energies at which they are observed, therefore, suggest the EGMF present exists at a non-negligible level. At such values, the EGMF can lead to an energy dependent broadening of the initial jet beam. With the lower energy cascade electrons being more strongly deflected by the EGMF, this beam broadening is largest for these electrons. Through the application of theoretical EM cascade models to the particular blazar 1ES 0229+200, an EGMF strength stronger than 10^{-17} G is suggested to be necessary in order to prevent conflict with both the *HESS* and *Fermi* blazar flux measurements, as has been noted previously in [25].

Furthermore, following a relaxation of the EBL normalisation put into this calculation, the excluded EGMF strength was found to vary significantly. A lower (higher) EBL normalisation lead to a reduced (increased) EGMF constraint. Though all EBL normalisations within the range best motivated by recent observations allow the EGMF to be bound, reducing the EBL normalisation by a factor of 0.85 can reduce the bound on the EGMF down to 10^{-18} G, as shown in Fig 7.

Such considerations provide new insights into the EGMF and reduce dramatically the available $\lambda_B - B$ parameter space. However, our limited knowledge in the temporal activity of these blazars to only the past several years severely restricts the use of spectral information in inferring EGMF constraints due to time delay effects.

Time delay limitations, however, do not plague angular profile investigations, for which $\sim$300 GeV γ-rays can allow an EGMF probe two orders of magnitude below those reachable by spectral studies. In this way, the constraints provided by the angular profile studies of blazars offer a complimentary new probe into the EGMF. We investigate whether signatures of blazar angular broadening exist for the particular case of PKS 2155-304, the blazar for which the highest number of photons are presently available. Preliminary results from this study indicate that a window in the $\lambda_B - B$ parameter space is excluded by the lack of any angular broadening feature at these energies. A plot summarising our new bounds on the EGMF utilising EM cascades from two architypal blazars is shown in Fig. 9.

REFERENCES

1. Kronberg P.P., 1994, Rept.Prog.Phys., 57, 325
2. Grasso D., Rubinstein H.R., 2001, Phys.Rept., 348, 163
3. Widrow L.M., 2002, Rev.Mod.Phys. 74, 775
4. Beck R., 2009, AIP Conf. Proc. 1085, 83
5. Kulsrud R.M., Zweibel E.G., 2008, Rept.Prog.Phys., 71, 0046091
6. Kronberg P.P., Simard-Normandin M., 1976 Nature, 263, 653
7. Kronberg P.P., Perry J.J., 1982, Ap.J., 263, 518
8. Blasi P., Burles S., Olinto A.V., 1999, Ap.J. 514, L79
9. Barrow J.D., Ferreira P.G. Silk J., 1997, Phys. Rev. Lett. 78, 3610
10. Durrer R., Ferreira P.G., Kahniashvili T., 2000, Phys.Rev. D 61, 043001
11. Aharonian F.A., Coppi P. Voelk H., 1994, Ap.J., 423, L5
12. Plaga R., 1995, Nature, 374, 430
13. Coppi P.S., Aharonian F.A., 1997, Ap.J., 487, L9
14. Neronov A., Semikoz D.V., 2007, JETP Lett., 85, 473, [arXiv:astro-ph/0604607]
15. Murase K., Takahashi K., Inoue S., Ichiki K., Nagataki S., 2008, Ap.J., 686, L67
16. Eungwanichayapant A., Aharonian F.A., 2009, Int.J. Mod.Phys. D 18, 911
17. Neronov A., Semikoz D.V., 2009, Phys.Rev. D 80, 123012
18. Elyiv A., Neronov A., Semikoz D.V., 2009, Phys. Rev. D, 80, 023010
19. Dolag K., Kachelriess M., Ostapchenko S. and Tomas R., 2009, Ap.J. 703, 1078
20. Neronov A., Vovk Ie., 2010, Science, 328, 73
21. Tavecchio F., Ghisellini G., Bonnoli G., Foschini L., 2010, arXiv:1009.1048
22. K. Dolag, M. Kachelriess, S. Ostapchenko and R. Tomas, arXiv:1009.1782
23. Dermer C.D., Cavadini M., Razzaque S., Finke J.D. Lott B., 2010, arXiv:1011.6660
24. Franceschini A., Rodighiero G. Vaccari M., A&A, 487, 837, 2008
25. Taylor A., Vovk Ie., Neronov A., A&A, volume 529, 2011
26. Dominguez A., Primack J.R., Rosario D.J. et al., MNRAS, volume 410, issue 4, pp. 2556-2578
27. Orr M., Krennrich F., Dwek E., ApJ, volume 733, issue 2, article id. 77 (2011)
28. A. Neronov and D. V. Semikoz, Phys. Rev. D **80** (2009) 123012 [arXiv:0910.1920 [astro-ph.CO]].
29. Aharonian F. et al., A&A, volume 475, L9, 2007
30. Dermer C., Cavadini M., Razzaque S., Finke J., Chiang J., Lott B., ApJ Letters, volume 733, issue 2, article id. L21, 2011
31. H. Huan, T. Weisgarber, T. Arlen and S. P. Wakely, arXiv:1106.1218 [astro-ph.HE].
32. Atwood W.B., 2009, Ap.J., 697, 1071
33. Abdo A.A. et al., 2011, arXiv:1108.1435
34. I. Vovk, A. M. Taylor, D. Semikoz and A. Neronov, arXiv:1112.2534 [astro-ph.CO].